Interfacial effect of polyacetylene-based polyelectrolyte on the performance of inverted PTB7:$PC_{71}BM$ solar cells

Sungho Nam,[1,2] Jooyeok Seo,[1] Myeonghun Song[1], Hwajeong Kim,[1,3] Moonhor Ree,[4] Yeong-Soon Gal,[5] Donal D. C. Bradley[2,6] and Youngkyoo Kim[1,a)]

[1]*Organic Nanoelectronics Laboratory, Department of Chemical Engineering, School of Applied Chemical Engineering, Kyungpook National University, Daegu 41566, Republic of Korea*

[2]*Department of Physics, Division of Mathematical, Physical and Life Sciences, University of Oxford, Oxford OX1 3PD, United Kingdom*

[3]*Research Institute of Advanced Energy Technology, Kyungpook National University, Daegu 41566, Republic of Korea*

[4]*Department of Chemistry, Division of Advanced Materials Science, Pohang University of Science and Technology, Pohang 37673, Republic of Korea*

[5]*Polymer Chemistry Laboratory, College of Engineering, Kyungil University, Gyeongsan 38428, Republic of Korea*

[6]*Department of Engineering Science, Division of Mathematical, Physical and Life Sciences, University of Oxford, Oxford OX1 3PD, United Kingdom*

We report the improved performance of inverted-type polymer:fullerene solar cells, of which the active layers are composed of poly[4,8-bis[(2-ethylhexyl)oxy]benzo[1,2-b:4,5-b']dithiophene-2,6-diyl][3-fluoro-2-[(2-ethylhexyl)carbonyl]thieno[3,4-b]-thiophenediyl] (PTB7) and [6,6]-phenyl C_{71}-butyric acid methyl ester ($PC_{71}BM$), by introducing poly(N-dodecyl-2-ethynylpyridiniumbromide) (PDEPB) interlayers between the active layers and the electron-collecting zinc oxide (ZnO) layers. The thickness of the PDEPB interlayers was controlled by varying the concentration of PDEPB solutions in methanol. Results showed that the power conversion efficiency (PCE) of the PTB7:$PC_{71}BM$ solar cells increased from 7.73% to 8.14% in the presence of the PDEPB interlayers prepared from 0.5 mg/mL PDEPB solutions. The improved PCE was attributed to the lowered work functions of ZnO, induced by the PDEPB layers (by Kelvin probe measurement), which was supported by the noticeable change in the atom environments of both the ZnO and PDEPB layers (by X-ray photoelectron spectroscopy measurement).

[a)]Electronic mail: ykimm@knu.ac.kr

Polymer solar cells (PSCs) with bulk heterojunction (BHJ) layers of conjugated polymers and fullerene derivatives have attracted widespread attention because large-area flexible plastic solar modules can be fabricated by employing continuous roll-to-roll (R2R) processes using polymeric solutions at low temperatures.[1-3] Recently, the power conversion efficiencies (PCE) of PSCs with a single-stack structure have been dramatically increased up to ~11%, which can be attributable to improved control of BHJ morphology, effective surface/interface engineering of buffer layers, and newly synthesized conjugated polymers.[4-10] The charge generation, recombination, and extraction in BHJ layers have also been investigated for a comprehensive understanding of these phenomena.[11-15]

Inverted-type PSCs, consisting of BHJ absorption layer sandwiched between the electron collecting buffer layer (ECBL) on the bottom electrode and the high-work-function top electrode, have shown superior efficiency compared to normal-type PSCs upon modifying the ECBL with an organic interfacial layer (interlayer).[12,16,17] This organic interfacial layer ensures better physical contact between the ECBLs and the BHJ layer.[18,19] It also plays an important role in lowering the work function of the metal oxide ECBL because of its dipole nature, thereby increasing the built-in potential (V_{BP}), and subsequently facilitating charge transport and enhancing the charge collection efficiency.[20,21]

To date, extensive studies on water/alcohol-soluble organic interfacial layer materials such as non-conjugated neutral polymers, conjugated polyelectrolytes, small molecules, and self-assembled monolayer molecules have been reported on account of their intriguing properties such as extraordinary solubility in highly polar solvents to enable multilayer film deposition, environment-friendly processing, and interface modification functions.[20,22-31] Very recently, we have reported the effect of a poly(N-dodecyl-2-ethynylpyridiniumbromide) (PDEPB) interlayer on the solar cell performance;[32] however, further studies using different materials are needed to confirm the influence of the PDEPB interlayer and to clarify the interplay between ECBL and PDEPB interlayer.

Herein, we studied the optical properties and the electronic structure of PDEPB polymer and examined the influence of the PDEPB dipole interlayer, which modifies the ZnO ECBL in inverted PSCs, on the PTB7:$PC_{71}BM$ solar cell performance by varying the PDEPB solution concentration. In addition, the changes in atom environment and work function of PDEPB-coated ZnO film were investigated by X-ray photoelectron spectroscopy (XPS) and Kelvin probe (KP) measurements.

PDEPB (viscosity = 0.14–0.22 dL g^{-1} in DMF at 25 °C) was synthesized as described in a previous report,[33,34] while zinc acetate dihydrate (purity > 99%) was supplied by Sigma-Aldrich (United States). PTB7 polymer (weight-average molecular weight = 92 kDa, polydispersity index = 2.6) and $PC_{71}BM$ (purity > 99%) were purchased from 1-Material (Canada) and

Nano-C (United States), respectively. The ZnO precursor solution was prepared by dissolving zinc acetate dihydrate (1 g) and ethanolamine (0.28 mL) in 2-methoxyethanol (10 mL), followed by stirring at 60 °C for 3 h and at room temperature overnight prior to spin-coating. The PDEPB solutions were prepared using methanol with different concentrations (0, 0.1, 0.3, 0.5, 0.7, and 1.0 mg/mL). PTB7:$PC_{71}BM$ (10:15 by weight) solutions were prepared using 97 vol% of chlorobenzene (CB) and 3 vol% of 1,8-diiodooctane (DIO) at a solid concentration of 25 mg/mL, and then were vigorously stirred at room temperature for 12 h before spin-coating. Pre-patterned indium-tin oxide (ITO)-coated glass substrates were cleaned by wet cleaning with acetone and isopropyl alcohol, followed by dry cleaning with UV-ozone treatment for 20 min. The 30-nm-thick ZnO films were spin-coated on the ITO-glass substrates and were annealed at 200 °C for 1 h. The PDEPB solutions were spin-coated onto the top of the ZnO layer, followed by thermal annealing at 120 °C for 15 min. The 100-nm-thick PTB7:$PC_{71}BM$ BHJ layers were spin-coated onto the ZnO/PDEPB layers in a nitrogen-filled glove box and were dried for 20 min. All samples were transferred to a vacuum chamber inside an argon-filled glove box. The 10-nm-thick molybdenum oxide (MoO_3) and 70-nm-thick silver (Ag) layers were sequentially deposited through a shadow mask under 2×10^{-6} Torr, defining the active area of 0.055 cm^{-2}. Devices were characterized using a solar cell and an external quantum efficiency (EQE) measurement system equipped with solar simulator (92250A-1000, Newport-Oriel), sourcemeter (Model 2400, Keithley), monochromator (CM110, Spectral Products), and light source (Tungsten-Halogen lamp, 150W, ASBN-W, Spectral Products). The core-level atom environments were measured with an X-ray photoelectron spectrometer (XPS, Theta Probe AR-XPS System, Thermo Fisher Scientific) with a monochromatic X-ray source of Al Kα (1486.6 eV). The ECBL work functions were also examined using a Kelvin probe measurement (APS01, KP Technology) under ambient conditions and were calibrated against highly ordered pyrolytic graphite.

Figure 1

Inverted PTB7:$PC_{71}BM$ BHJ solar cells with PDEPB interlayer were fabricated as shown in Fig. 1a. The PDEPB solution concentration was varied from 0 to 1 mg/mL in methanol, to investigate the correlation between solution concentration (which, in turn, is related to layer thickness) and solar cell performance. The PDEPB thin film showed a strong absorption peak at ~510 nm with a long tail (see Fig. 1b) and the optical bandgap of the PDEPB polymer—estimated from the Tauc plot (see the inset of Fig. 1b)—was ~2.0 eV. The photoelectron yield (PEY) spectrum of the PDEPB polymer revealed the highest occupied molecular orbital (HOMO) energy level of −5.6 eV (see Fig. 1c). The onset point of the

polymer should be calibrated as previously described and the PTB7 film was used as a reference for calibration.[35] The lowest unoccupied molecular orbital (LUMO) energy level of −3.6 eV for the PDEPB polymer was calculated from the optical bandgap and the HOMO energy level. Therefore, we summarized the energy band structure of the PDEPB polymer as illustrated in the inset of Fig. 1c.

Figure 2

The current density-voltage (J-V) curves under simulated solar light (air mass 1.5G, 100 mW/cm^2) are shown in Fig. 2a. The control device with bare ZnO layer (ITO/ZnO/PTB7:$PC_{71}BM$:MoO_3/Ag) exhibited a relatively low short circuit current density (J_{SC}). However, better device performances were obtained for the device with ZnO/PDEPB_0.5 layer (ITO/ZnO/PDEPB_0.5/PTB7:$PC_{71}BM$:MoO_3/Ag), which is in good agreement with a previous report.[32] Upon increasing the PDEPB solution concentration further (> 0.5 mg/mL), the device performance worsened due to the gradual decrease in J_{SC}. To confirm the enhanced J_{SC} of the device with the ZnO/PDEPB_0.5 layer, we measured the EQE spectra of the devices (see the inset of Fig. 2a). Notably, the higher EQE values of the device with ZnO/PDEPB_0.5 layer than those of the control device and the device with ZnO/PDEPB_1.0 (ITO/ZnO/PDEPB_1.0/PTB7:$PC_{71}BM$:MoO_3/Ag) were shown for the spectral range of 350–600 nm, indicating that the photogenerated charges were more efficiently transported and collected at the respective electrodes. Here we note that 0.5 and 1.0 mg/mL PDEPB data are labelled as PDEPB_0.5 and PDEPB_1.0, respectively. Solar cell parameters as a function of PDEPB solution concentration are shown in Fig. 2b. As the PDEPB solution concentration increased up to 0.5 mg/mL, the V_{OC}, J_{SC}, and fill factor (FF) values increased gradually. As a result, the device with the ZnO/PDEPB_0.5 layer exhibited noticeably improved PCE of 8.14% with V_{OC} = 722 mV, J_{SC} = 16.06 mA/cm^2, and FF = 70.18%, compared to control device with PCE = 7.73% (V_{OC} = 711 mV, J_{SC} = 15.58 mA/cm^2, and FF = 69.44%). However, the solar cell performance worsened when PDEPB solution concentration increased beyond 0.5 mg/mL because of gradually decreasing V_{OC}, J_{SC}, and FF values. Therefore, the PDEPB solution concentration could play a significantly important role in determining the device performance.

Figure 3

In order to gain insight into the chemical interaction between the ZnO layer and the PDEPB interlayer at 0.5 mg/mL, we performed XPS measurement (Fig. 3). The Zn 2p core-level spectra of the bare ZnO and ZnO/PDEPB_0.5 layer indicated the presence of PDEPB interlayer on the ZnO layer, based on the decreased Zn 2p peak intensity for ZnO/PDEPB_0.5 layer compared to that for the bare ZnO layer. It is further evidenced by the N 1s peaks at 398.5 and 400 eV, corresponding to the protonated N atoms of the pyridine rings and N^+ groups of the pyridinium cations in the PDEPB polymer, respectively.[36] Particularly, the Zn 2p peaks shifted toward a lower binding energy by 0.3 eV (from 1044.9 and 1021.8 eV to 1044.6 and 1021.5 eV) because of the presence of higher electron densities around the Zn atoms.[37] Additionally, the chemical interaction between the Zn cations and the bromide anions for the ZnO/PDEPB_0.5 layer was observed based on the binding energies of 68.8 and 69.8 eV, which is in good agreement with a previous report (here we note that the peaks at 67.5 and 68.2 eV could be associated with free bromide anions).[38] This result indicated that the Zn atoms could be coordinated with the bromide anions in PDEPB polymer, indicating that the defects on the ZnO surface could be reduced by the presence of the PDEPB polymer, leading to enhancement in charge extraction efficiency. Considering the incorporation of Zn with Br, we can expect that the electronic structure of the ZnO layer could be changed by the presence of the PDEPB polymer.

Figure 4

We further performed KP measurement to analyze the change in the ZnO work function with and without PDEPB interlayers. Fig. 4a shows that the work function of the bare ZnO layer was 4.51 eV, while it decreased to 4.18 eV and further to 4.09 eV for the ZnO/PDEPB_0.5 and ZnO/PDEPB_1.0 layers, respectively. This reduced work function can be closely related with the PDEPB dipole layer and the increased V_{BP}. Hence, these results suggest that the increased charge (electron) extraction efficiency and reduction in charge recombination loss due to the presence of the PDEPB_0.5 layer can be mainly ascribed to the increased V_{BP}, leading to enhanced device performance using the ZnO/PDEPB_0.5 layer. Furthermore, as shown by the dark J-V curves in Fig. 4b, enhanced device performance can also be attributed to the improved charge transport for the device with the ZnO/PDEPB_0.5 layer, based on the higher rectification ratio resulting from low leakage current. This leads to higher J_{SC} and FF values compared to the control device and the device with the ZnO/PDEPB_1.0 layer (here we note that the rectification ratios are 97, 2214, and 226 for the control device, device with ZnO/PDEPB_0.5 layer, and device with ZnO/PDEPB_1.0 layer, respectively). However, the relatively thick ZnO/PDEPB_1.0 layer could provide the

leakage current pathway, resulting in relatively poor device performance despite the reduced work function of the ZnO/PDEPB_1.0 layer.

In conclusion, we have demonstrated the influence of the PDEPB interfacial dipole layer on the inverted PTB7:$PC_{71}BM$ solar cell performance. Inverted PTB7:$PC_{71}BM$ solar cells with 0.5 mg/mL PDEPB solution coated on ZnO ECBL achieved a PCE of 8.14%, which is higher than that of the control device with bare ZnO layer and the device with a ZnO/PDEPB_1.0 layer. Surface defects on the ZnO ECBL can be cured by the presence of the PDEPB interlayer, confirmed by Zn–Br chemical interaction. This improvement in PCEs can also be attributed to the reduced work function of the ZnO/PDEPB_0.5 layer, resulting in increased V_{BP}, which facilitates overall charge transport. Hence our present study provides a promising method for improving the solar cell performance, realizing the portable and wearable energy conversion devices.

ACKNOWLEDGMENTS

This work was financially supported by Korean Government grants (NRF_2015R1A2A2A01003743, NRF_2016H1D5A1910319, NRF_2014R1A1A3051165, Human Resource Training Project for Regional Innovation, MOE and NRF-2014H1C1A1066748, and Basic Science Research Program_2009-0093819).

REFERENCES

1. R. R. Søndergaard, M. Hösel, D. Angmo, T. T. Larsen-Olsen, and F. C. Krebs, Mater. Today, **15**, 36 (2012).
2. D. Angmo, T. T. Larsen-Olsen, M. Jørgensen, R. R. Søndergaard, and F. C. Krebs, Adv. Energy Mater., **3**, 172 (2013).
3. S. Hong, H. Kang, G. Kim, S. Lee, S. Kim, J. H. Lee, J. Lee, M. Yi, J. Kim, H. Back, J. R. Kim, and K. Lee, Nat. Commun., **7**, 10279 (2016).
4. S. Li, L. Ye, W. Zhao, S. Zhang, S. Mukherjee, H. Ade, and J. Hou, Adv. Mater., **28**, 9423 (2016).
5. J. Zhao, Y. Li, G. Yang, K. Jiang, H. Lin, H. Ade, W. Ma, and H. Yan, Nat. Energy, **1**, 15027 (2016).
6. D. Baran, R. S. Ashraf, D. A. Hanifi, M. Abdelsamie, N. Gasparini, J. A. Rohr, S. Holliday, A. Wadsworth, S. Lockett, M. Neophytou, C. J. Emmott, J. Nelson, C. J. Brabec, A. Amassian, A. Salleo, T. Kirchartz, J. R. Durrant, and I. McCulloch, Nat. Mater., doi: 10.1038/nmat4797 (2016).
7. M. Campoy-Quiles, T. Ferenczi, T. Agostinelli, P. G. Etchegoin, Y. Kim, T. D. Anthopoulos, P. N. Stavrinou, D. D. Bradley, and J. Nelson, Nat. Mater., **7**, 158 (2008).

8. Y. Kim, S. Cook, S. M. Tuladhar, S. A. Choulis, J. Nelson, J. R. Durrant, D. D. C. Bradley, M. Giles, I. McCulloch, C.-S. Ha, and M. Ree, Nat. Mater., **5**, 197 (2006).
9. H.-Y. Chen, J. Hou, S. Zhang, Y. Liang, G. Yang, Y. Yang, L. Yu, Y. Wu, and G. Li, Nat. Photon., **3**, 649 (2009).
10. Y. Liang, Z. Xu, J. Xia, S. T. Tsai, Y. Wu, G. Li, C. Ray, and L. Yu, Adv. Mater., **22**, E135 (2010).
11. I. Fraga Domínguez, A. Distler, and L. Lüer, Adv. Energy Mater., doi: 10.1002/aenm.201601320 (2016).
12. L. Lu, T. Zheng, Q. Wu, A. M. Schneider, D. Zhao, and L. Yu, Chem. Rev., **115**, 12666 (2015).
13. S. M. Ryno, M. K. Ravva, X. Chen, H. Li, and J.-L. Brédas, Adv. Energy Mater., doi: 10.1002/aenm.201601370 (2016).
14. D. M. Stoltzfus, J. E. Donaghey, A. Armin, P. E. Shaw, P. L. Burn, and P. Meredith, Chem. Rev., **116**, 12920 (2016).
15. S. R. Cowan, N. Banerji, W. L. Leong, and A. J. Heeger, Adv. Funct. Mater., **22**, 1116 (2012).
16. G. Li, C. W. Chu, V. Shrotriya, J. Huang, and Y. Yang, Appl. Phys. Lett., **88**, 253503 (2006).
17. S. K. Hau, H.-L. Yip, N. S. Baek, J. Zou, K. O'Malley, and A. K. Y. Jen, Appl. Phys. Lett., **92**, 253301 (2008).
18. Y.-J. Cheng, C.-H. Hsieh, Y. He, C.-S. Hsu, and Y. Li, J. Am. Chem. Soc., **132**, 17381 (2010).
19. S. K. Hau, H.-L. Yip, O. Acton, N. S. Baek, H. Ma, and A. K. Y. Jen, J. Mater. Chem., **18**, 5113 (2008).
20. J.-H. Lee, B. H. Lee, S. Y. Jeong, S. B. Park, G. Kim, S. H. Lee, and K. Lee, Adv. Energy Mater., **5**, 1501292 (2015).
21. Y. E. Ha, M. Y. Jo, J. Park, Y.-C. Kang, S. I. Yoo, and J. H. Kim, J. Phys. Chem. C, **117**, 2646 (2013).
22. C. Duan, C. Zhong, C. Liu, F. Huang, and Y. Cao, Chem. Mater., **24**, 1682 (2012).
23. W.-Y. Jin, R. T. Ginting, S.-H. Jin, and J.-W. Kang, J. Mater. Chem. A, **4**, 3784 (2016).
24. H. Kang, S. Hong, J. Lee, and K. Lee, Adv. Mater., **24**, 3005 (2012).
25. C. Liu, L. Zhang, L. Xiao, X. Peng, and Y. Cao, ACS Appl. Mater. Interfaces, **8**, 28225 (2016).
26. S. Nam, J. Seo, S. Woo, W. H. Kim, H. Kim, D. D. Bradley, and Y. Kim, Nat. Commun., **6**, 8929 (2015).
27. K. Sun, B. Zhao, A. Kumar, K. Zeng, and J. Ouyang, ACS Appl. Mater. Interfaces, **4**, 2009 (2012).
28. S. Woo, W. Hyun Kim, H. Kim, Y. Yi, H.-K. Lyu, and Y. Kim, Adv. Energy Mater., **4**, 1301692 (2014).
29. T. Yang, M. Wang, C. Duan, X. Hu, L. Huang, J. Peng, F. Huang, and X. Gong, Energy Environ. Sci., **5**, 8208 (2012).
30. K. Zhang, C. Zhong, S. Liu, C. Mu, Z. Li, H. Yan, F. Huang, and Y. Cao, ACS Appl. Mater. Interfaces, **6**, 10429 (2014).

31. M. Jin Tan, S. Zhong, R. Wang, Z. Zhang, V. Chellappan, and W. Chen, Appl. Phys. Lett., **103**, 063303 (2013).
32. S. Nam, J. Seo, H. Han, H. Kim, S. G. Hahm, M. Ree, Y.-S. Gal, T. D. Anthopoulos, D. D. C. Bradley, and Y. Kim, Adv. Mater. Interfaces, doi:10.1002/admi.201600415 (2016).
33. K. T. Lim, S. H. Jin, H. J. Lee, J. W. Park, S. Y. Kim, W. C. Lee, and Y. S. Gal, Syn. Met., **153**, 301 (2005).
34. Y.-S. Gal, S.-H. Jin, J.-W. Park, K. T. Lim, K. Koh, S. C. Han, and J. W. Lee, Curr. Appl. Phys., **7**, 517 (2007).
35. S. Nam, M. Shin, H. Kim, C.-S. Ha, M. Ree, and Y. Kim, Adv. Funct. Mater., **21**, 4527 (2011).
36. C. Yao, X. Li, K. G. Neoh, Z. Shi, and E. T. Kang, J. Membr. Sci., **320**, 259 (2008).
37. Y. Wang, H. Fu, Y. Wang, L. Tan, L. Chen, and Y. Chen, Phys. Chem. Chem. Phys., **18**, 12175 (2016).
38. K. Kim, M. Suh, J. Choi, D. Lee, Y. Kim, S. H. Cheong, D. Kim, and D. Y. Jeon, Adv. Funct. Mater., **25**, 7450 (2015).

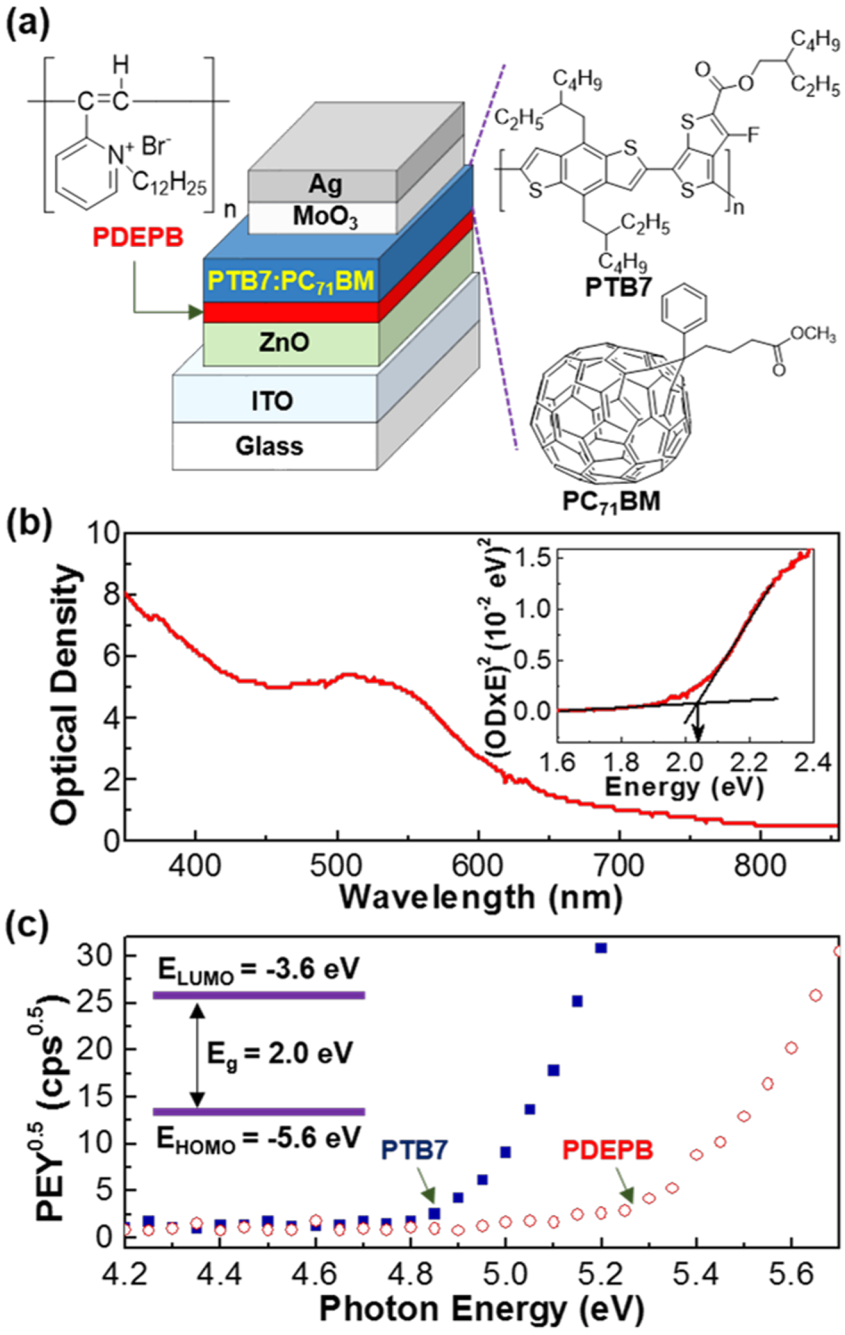

FIG. 1 (a) Device structure for the inverted polymer solar cell with the PDEPB interlayer and the PTB7:$PC_{71}BM$ BHJ layer. (b) Optical absorption spectrum for the PDEPB thin film coated on quartz substrate (inset: Tauc plot for band gap determination). (c) Photoelectron yield (PEY) spectra for the pristine PDEPB and PTB7 films coated on ITO-glass substrates (inset: a simplified energy band diagram for the PDEPB polymer).

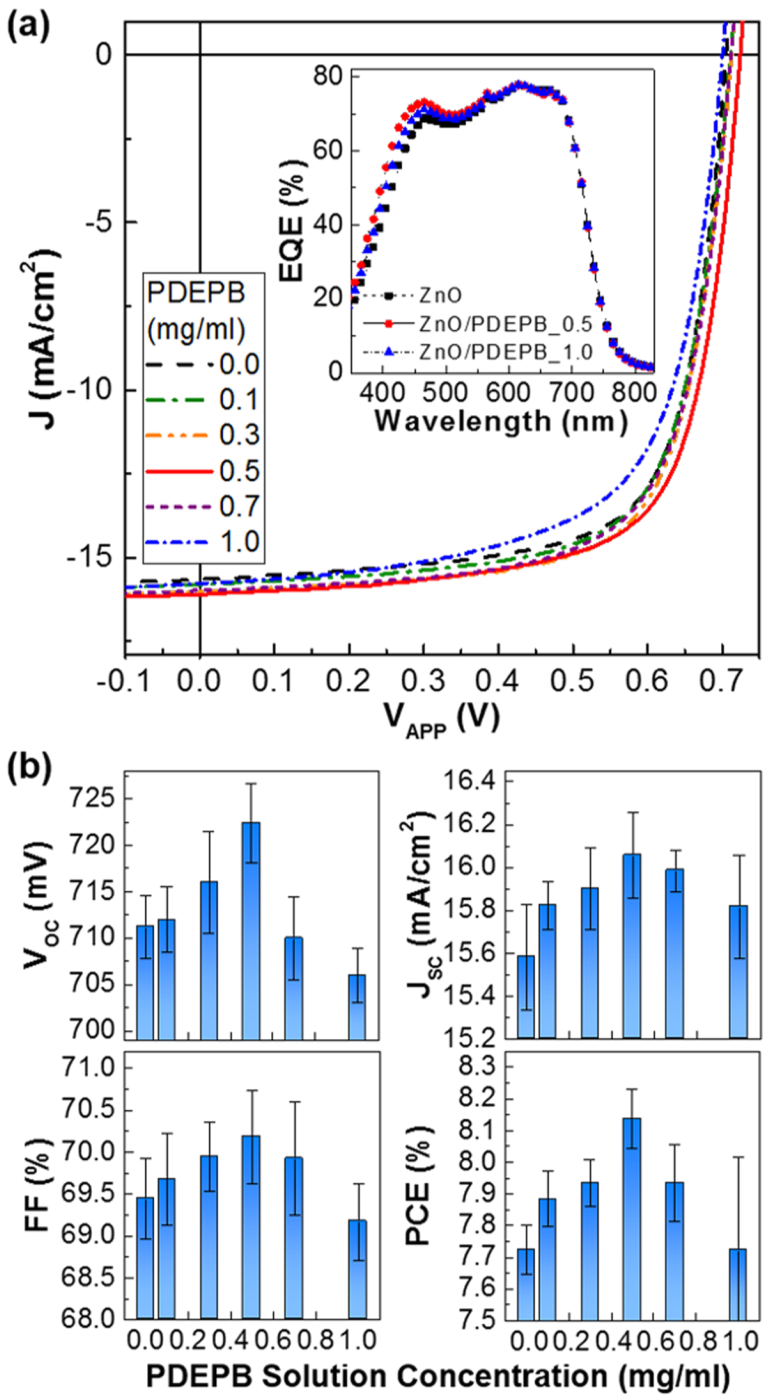

FIG. 2 (a) Light (air mass 1.5G, 100 mW/cm^2) J-V curves for the inverted-type PTB7:$PC_{71}BM$ solar cells with the PDEPB interlayers according to the various PDEPB solution concentrations (inset: EQE spectra). (b) Solar cell parameters as a function of PDEPB solution concentration.

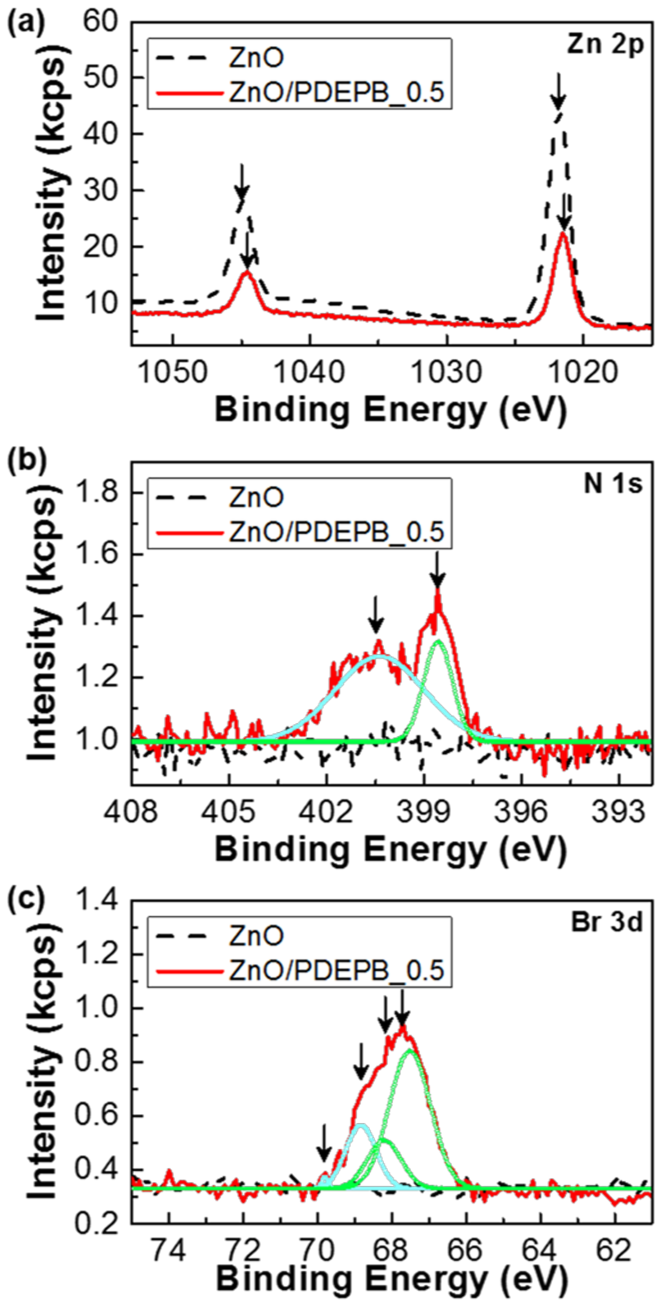

FIG. 3 XPS spectra for the ZnO-coated ITO-glass substrate and the PDEPB (0.5 mg/ml) layer-coated ZnO layer on the ITO-glass substrate: (a) Zn 2p, (b) N 1s, and (c) Br 3d.

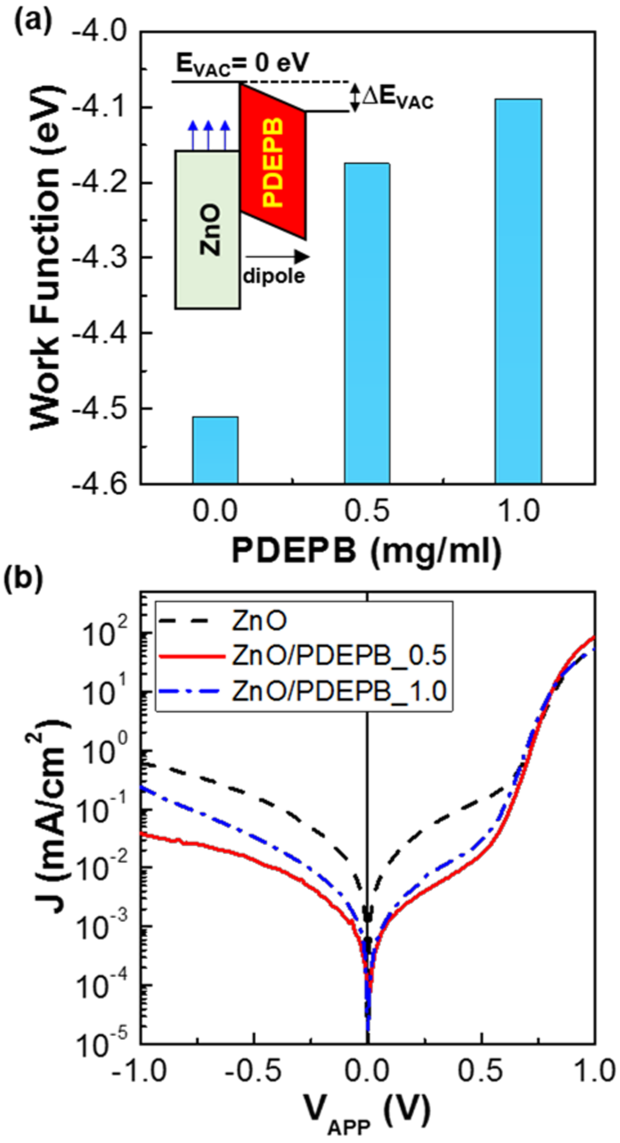

FIG. 4 (a) Change of ZnO work function (measured by Kelvin probe) according to the PDEPB concentration (inset: illustration for the ZnO work function shift by the presence of the PDEPB layer). (b) Dark J-V curves for the inverted-type PTB7:$PC_{71}BM$ solar cells according to the PDEPB concentration: 0 mg/ml (ZnO), 0.5 mg/ml (ZnO/PDEPB_0.5), and 1.0 mg/ml (ZnO/PDEPB_1.0).